Realistic Modeling of Complex Oxide Materials

I. V. Solovyev

Computational Materials Science Center, National Institute for Materials Science,
1-2-1 Sengen, Tsukuba, Ibaraki 305-0047, Japan

Abstract

Since electronic and magnetic properties of many transition-metal oxides can be efficiently controlled by external factors such as the temperature, pressure, electric or magnetic field, they are regarded as promising materials for various applications. From the viewpoint of electronic structure, these phenomena are frequently related to the behavior of a small group of states close to the Fermi level. The basic idea of this project is to construct a low-energy model for the states near the Fermi level on the basis of first-principles density functional theory, and to study this model by modern many-body techniques. After a brief review of the method, the abilities of this approach will be illustrated on a number of examples, including multiferroic manganites and spin-orbital-lattice coupled phenomena in RVO$_3$ (R being the three-valent element).

Keywords: first-principles calculations, effective models, transition-metal oxides
PACS: 71.15.-m, 71.10.Fd, 75.47.Lx, 71.10.-w

1. Basic Idea, Purpose, and Methods of Realistic Modeling

The oxide materials can be rather complex. Nevertheless, in many cases their electronic and magnetic properties are controlled by a small group of states located near the Fermi level and well isolated from the rest of the spectrum. A typical example of the electronic structure of YVO_3, obtained in the local-density approximation (LDA), is shown in Fig. 1. In this

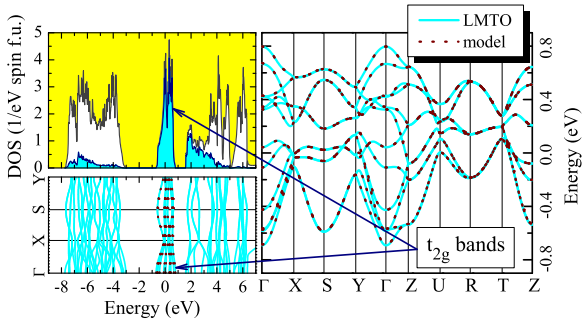

Figure 1: (Left panel) Electronic structure of orthorhombic YVO_3 in LDA. The shaded area shows the contributions of the 3d states of V. (Right panel) Enlarged behavior of t_{2g} bands computed from LMTO basis functions (solid curves) and downfolded bands (dot-dashed curves). The corresponding bands in the left panel are shown by arrows. The Fermi level is at zero energy.

case, the active states are twelve t_{2g} bands of predominantly V-character, which are separated by finite energy windows from other states, both from below and from above. Such a division of the entire electronic structure into the "active" and "inactive" (or low- and high-energy) states opens a formal way for combining the first-principles calculations, based on the density-functional theory (DFT), with the many-body treatment of some effective model, formulated rigorously in the restricted Hilbert space of "active" states. This is the main idea of realistic modeling of complex oxide materials. The purpose of this project is twofold:

(1) To incorporate the physics of Coulomb correlations, which is greatly oversimplified in conventional LDA;

(2) To provide a transparent physical picture for electronic and magnetic properties of complex compounds. In this sense, the realistic modeling can be regarded as supplementary approach to more conventional first-principles electronic structure calculations, which are currently on the rise.

Thus, the first step of the project is construction of the low-energy model (typically, the multiorbital Hubbard model) for the states near the Fermi level:

$$\hat{\mathcal{H}} = \sum_{\mathbf{R}\mathbf{R}'} \sum_{\alpha\beta} t^{\alpha\beta}_{\mathbf{R}\mathbf{R}'} \hat{c}^{\dagger}_{\mathbf{R}\alpha} \hat{c}_{\mathbf{R}'\beta} + \frac{1}{2} \sum_{\mathbf{R}} \sum_{\alpha\beta\gamma\delta} U_{\alpha\beta\gamma\delta} \hat{c}^{\dagger}_{\mathbf{R}\alpha} \hat{c}^{\dagger}_{\mathbf{R}\gamma} \hat{c}_{\mathbf{R}\beta} \hat{c}_{\mathbf{R}\delta}, \quad (1)$$

which would include the effect of other ("inactive") states in the definition of the model parameters of the Hamiltonian (1). All these parameters are derived totally from the "first-principles" on the basis of DFT. We would like to emphasize that, although the derivations are inevitably based on some approximations, we do not use any adjustable parameters apart from these approximations. The procedure of constructing the model Hamiltonian was described in details in the review article [1]. Briefly, in order to derive the one-electron part ($t^{\alpha\beta}_{\mathbf{R}\mathbf{R}'}$), we use the generalized downfolding method. For the isolated low-energy bands, this procedure is exact, as it is clearly seen in Fig. 1 from the comparison of the original band structure, obtained in the linear muffin-tin orbital method (LMTO) [2], and the one after the downfolding. The parameters of screened Coulomb interactions ($U_{\alpha\beta\gamma\delta}$) are typically obtained by combining the constrained DFT technique [3] with the random-phase approxima-

Email address: SOLOVYEV.Igor@nims.go.jp (I. V. Solovyev)

tion [4]. The latter is very efficient for treating the screening of correlated electrons by themselves [5], which can dramatically reduce the effective Coulomb interactions in the low-energy bands. For example, the bare Coulomb repulsion between 3*d* electrons is about 20-25 eV. However, for the low-energy bands in solids this value is typically reduced till 2-4 eV [1].

Once the model is constructed, it can be solved by using various many-body techniques. In the present work, we typically start with the mean-field Hartree-Fock (HF) approximation, and take into account the correlation interactions by considering the perturbation theory expansion near the HF ground state. This procedure may be justified, if the degeneracy of the ground state is lifted by the crystal distortions [1].

Below, we present examples of realistic modeling for two types of transition-metal oxides.

2. Spin-Orbital-Lattice Coupling in vanadates RVO$_3$

The vanadates RVO$_3$ (where R is the three-valent, typically rare-earth, element) have attracted a considerable experimental and theoretical attention. All these compounds crystallize in the distorted perovskite structure. For example, considered in the present work YbVO$_3$ can have orthorhombic and monoclinic modifications, realized at T= 15 and 75 K, respectively. However, a relatively small change of the lattice parameters may cause a dramatic reconstruction of electronic, and associated to it, magnetic structure. For example, at T= 15 and 75 K YbVO$_3$ forms the so-called G- and C-type antiferromagnetic (AFM) structure, respectively (Fig. 2). The phenomenon

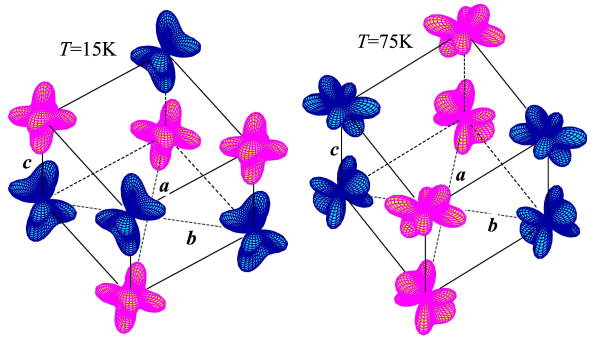

Figure 2: Distribution of the charge densities associated with the occupied t_{2g} orbitals (the orbital ordering) realized in the orthorhombic (left) and monoclinic (right) phase of YbVO$_3$ in the HF approximation. Different magnetic sublattices associated with two opposite directions of spins in the AFM structure are shown by different colors.

called "spin-orbital-lattice coupling" and is typically regarded as the test for various theories of the electronic structure. First attempts of realistic modeling of RVO$_3$ are summarized in [1]. After that we have performed a systematic study for the entire series RVO$_3$ (R= La, Ce, Pr, Nd, Sm, Gd, Tb, Ho, Yb, Lu, and Y), using the experimental crystal structure available in the literature [6, 7]. For all considered compounds, the effective Hubbard model was constructed for t_{2g} bands (Fig. 1) in the basis of three Wannier orbitals per each V-site. The details will be published elsewhere. Here we present an example of the "canonical behavior" realized in YbVO$_3$, where the crystal distortion quenches the orbital structure in some particular configuration (Fig. 2), which uniquely defines the type of the magnetic ground state, basically via Goodenough-Kanamori rules. In this case, once the degeneracy of t_{2g}-levels is lifted by the crystal distortion, the correct type of the magnetic ground state can be successfully reproduced already at the level of HF approximation. For example, the stabilization energy is clearly the largest for the experimentally observed G- and C-type AFM states when YbVO$_3$ crystallizes in the orthorhombic and monoclinic structure, respectively (Fig. 3). Moreover, the correct AFM ground

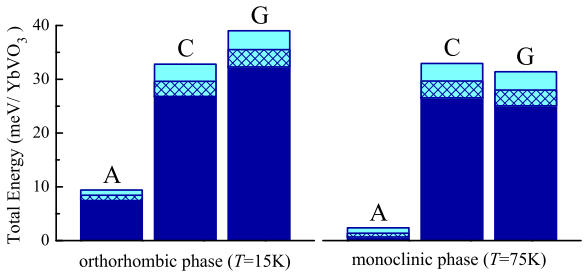

Figure 3: Stabilization energies of the main AFM states in YbVO$_3$ relative to the ferromagnetic state as obtained in the HF approximation (dark blue area) and after taking into account the correlation interactions in the second order of perturbation theory (light blue area) and in the t-matrix theory (hatched area).

state is additionally stabilized by correlation interactions, which are taken into account via perturbation-theory expansion near the HF solutions. We have considered two such technique for the total energy [8]: one is the regular second-order perturbation theory and the other one is the t-matrix theory. Both of them provide very consistent explanation for YbVO$_3$, although the correlation energies obtained in the t-matrix theory for the AFM states are systematically smaller due to the higher-order correlation effects, which are included to the t-matrix, but not to the second-order perturbation theory.

3. Inversion Symmetry Breaking in Manganites RMnO$_3$

The multiferroic manganites, such as BiMnO$_3$ and TbMnO$_3$, are currently under very intensive investigation. The multiferroicity means that the magnetic order in certain system without the inversion symmetry coexists with some finite ferroelectric polarization. The coupling of these two order parameters provides a unique opportunity to control the magnetic properties by applying the electric field and vice versa. From this point of view, the most interesting is the situation, where the inversion symmetry is broken by the magnetic degrees of freedom. In order to study the microscopic origin of the inversion symmetry breaking in manganites, we have constructed the effective model in the basis of three t_{2g} and two e_g orbitals at each Mn-site [9, 10]. The main results can be summarized as follows.

The mechanism of the inversion symmetry breaking is related to the behavior of interatomic magnetic interactions, which depends on the distribution of occupied e_g orbitals (Fig. 4). Although the orbital ordering differs dramatically in monoclinic and orthorhombic manganites, the basic idea is rather generic: the nearest-neighbor interactions J_{NN} always

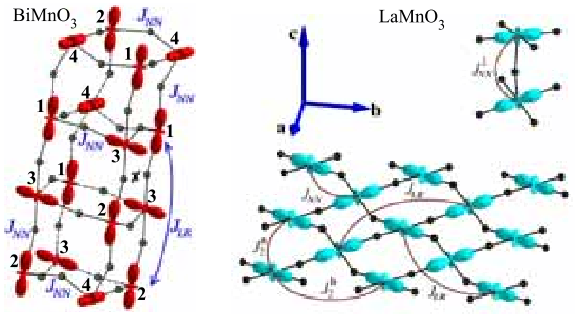

Figure 4: Typical distribution of the charge densities associated with the occupied e_g orbitals (the orbital ordering) realized in the monoclinic ($BiMnO_3$, left) and orthorhombic ($LaMnO_3$, right) manganites with the notations of main magnetic interactions.

compete with some long-range AFM interactions J_{LR}. The existence of J_{LR} is related to the fact that, due to the screening, the on-site Coulomb repulsion U is not particularly large (about 2.2 eV in manganites). Therefore, other mechanisms of magnetic interactions, besides conventional superexchange (being of the order of $1/U$), can be also operative. These mechanisms, which are of the higher orders than $1/U$, together with the form of the orbital ordering, naturally explain the large values of J_{LR} in some particular bonds [9]. When J_{LR} becomes larger than J_{NN}, they can lead to the formation of complex magnetic structures with the broken inversion symmetry. In monoclinic $BiMnO_3$, this is the collinear AFM structure, where each of the two sublattices (1,2) and (3,4) are coupled antiferromagnetically (see Fig. 4 for the notations of Mn-sites) [10]. In $TbMnO_3$, the ground state is the incommensurate spin-spiral, where the directions of spins in the **ab**-planes vary as $\mathbf{e_R}$=(cos **qR**, sin **qR**, 0), and the spin moments between the planes are coupled antiferromagnetically. Such a magnetic structure can be easily calculated by using the generalized Bloch theorem, which combines the lattice translations with the spin rotations [11]. The total energy minimum corresponds to the propagation along the orthorhombic **b**-axis, in agreement with the experiment. However, the obtained value q_b=0.675 (in units π/b, Fig. 5), is substantially larger than experimental q_b= 0.25 [12] and 0.28 [13], reported for magnetic structures with the moments lying in the **ab**- and **bc**-plane, respectively.

In order to resolve this discrepancy, we consider the relativistic spin-orbit interaction (SOI). In $BiMnO_3$, the SOI is responsible for the spin canting away from the collinear AFM structure and formation of the net ferromagnetic moment. Thus, the ferroelectric response in $BiMnO_3$, caused by the hidden AFM order, coexists with the ferromagnetism and can be controlled by the magnetic field [10]. The magnetic interactions of the relativistic origin play an important role also in $TbMnO_3$ [14]. In the search for the true magnetic ground state of $TbMnO_3$, we have investigated several magnetic structures with different periodicity. The structure corresponding to the lowest energy is shown in Fig. 6. The periodicity of this structure is described by q_b=0.25, in agreement with the experiment [12]. Nevertheless, it is no longer the uniform spin-spiral. It would be interesting to check our finding experimentally.

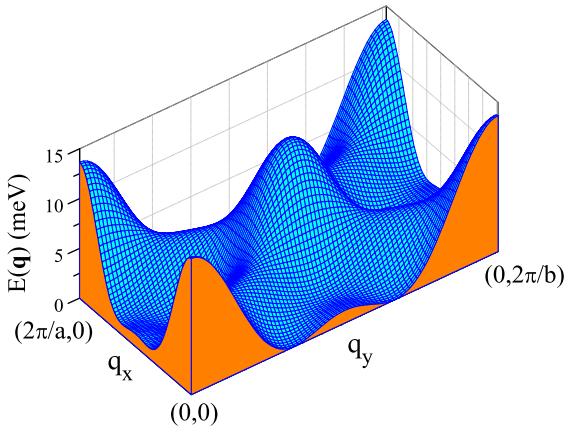

Figure 5: Dependence of the total energy (measured in meV per one formula unit) on the homogeneous spin-spiral vector **q** obtained in the Hartree-Fock approximation for $TbMnO_3$ without the relativistic spin-orbit coupling.

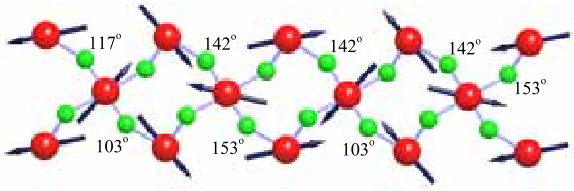

Figure 6: Distribution of magnetic moments in the **ab**-plane obtained in the HF approximation with SOI for $TbMnO_3$. The angles formed by Mn-moments in the bonds Mn-O-Mn are specified by numbers.

4. Conclusions

The realistic modeling combines the accuracy and predictable power of first-principles electronic structure calculations with the flexibility and insights of the model analysis. The first applications of this method are very encouraging. We hope that these ideas will continue to develop to become a powerful tool for theoretical analysis of complex oxide materials and other strongly correlated systems.

Acknowledgment

The work is partly supported by Grant-in-Aid for Scientific Research (C) No. 20540337 and in Priority Area “Anomalous Quantum Materials” from the Ministry of Education, Culture, Sport, Science and Technology of Japan.

[1] I.V. Solovyev, J. Phys.: Condens. Matter 20 (2008) 293201.
[2] O.K. Andersen, Phys. Rev. B 12 (1975) 3060.
[3] P.H. Dederichs et al., Phys. Rev. Lett. 53 (1984) 2512.
[4] F. Aryasetiawan et al., Phys. Rev. B 70 (2004) 195104.
[5] I.V. Solovyev, Phys. Rev. Lett. 95 (2005) 267205.
[6] M.H. Sage, Orbital, charge and magnetic order of RVO_3 perovskites, Ph.D. thesis, the University of Gronongen, the Netherland, 2006.
[7] G.R. Blake, private communication, 2007.
[8] I.V. Solovyev, J. Exp. Theor. Phys. 105 (2007) 46.
[9] I. Solovyev, J. Phys. Soc. Jpn. 78 (2009) 054710.
[10] I.V. Solovyev, Z.V. Pchelkina, J. Exp. Theor. Phys. Letters 89 (2009) 701.
[11] L.M. Sandratskii, Phys. Status Sol. B 136 (1986) 180.
[12] T. Arima et al., Phys. Rev. B 72 (2005) 100102.
[13] T. Kimura et al., Nature 426 (2003) 55.
[14] M. Mochizuki, N. Furukawa, J. Phys. Soc. Jpn. 78 (2009) 053704.